Measurement of the $D^{*\pm}$ Cross Section in Two Photon Collisions at LEP

The ALEPH Collaboration*

Abstract

The inclusive production of $D^{*\pm}$ mesons in photon-photon collisions has been measured by the Aleph experiment at LEP with a beam energy of 45 GeV. The D^{*+} are detected in their decay to $D^0\pi^+$ with the D^0 observed in three separate decay modes: (1) $K^-\pi^+$, (2) $K^-\pi^+\pi^0$ and (3) $K^-\pi^+\pi^-\pi^+$, and analagously for D^{*-} modes. A total of 33 events was observed from an integrated luminosity of 73 pb^{-1} which corresponds to a cross section for $\sigma(e^+e^- \rightarrow e^+e^- D^{*\pm}X)$ of $155 \pm 33 \pm 21$ pb. This result is compatible with both the direct production $\gamma\gamma \rightarrow c\bar{c}$ in the Born approximation and with a more complete calculation which includes both radiative QCD corrections and contributions in which one of the photons is first resolved into its quark and gluon constituents. The shapes of distributions for events containing a D^{*+} are found to be better described by the latter.

(Submitted to Physics Letters B)

---

* See next pages for the list of authors

The ALEPH Collaboration

D. Buskulic, D. Casper, I. De Bonis, D. Decamp, P. Ghez, C. Goy, J.-P. Lees, M.-N. Minard, P. Odier, B. Pietrzyk

Laboratoire de Physique des Particules (LAPP), IN^2P^3-CNRS, 74019 Annecy-le-Vieux Cedex, France

F. Ariztizabal, M. Chmeissani, J.M. Crespo, I. Efthymiopoulos, E. Fernandez, M. Fernandez-Bosman, V. Gaitan, Ll. Garrido,[15] M. Martinez, S. Orteu, A. Pacheco, C. Padilla, F. Palla, A. Pascual, J.A. Perlas, F. Sanchez, F. Teubert

Institut de Fisica d'Altes Energies, Universitat Autonoma de Barcelona, 08193 Bellaterra (Barcelona), Spain[7]

D. Creanza, M. de Palma, A. Farilla, G. Iaselli, G. Maggi,[3] N. Marinelli, S. Natali, S. Nuzzo, A. Ranieri, G. Raso, F. Romano, F. Ruggieri, G. Selvaggi, L. Silvestris, P. Tempesta, G. Zito

Dipartimento di Fisica, INFN Sezione di Bari, 70126 Bari, Italy

X. Huang, J. Lin, Q. Ouyang, T. Wang, Y. Xie, R. Xu, S. Xue, J. Zhang, L. Zhang, W. Zhao

Institute of High-Energy Physics, Academia Sinica, Beijing, The People's Republic of China[8]

G. Bonvicini, M. Cattaneo, P. Comas, P. Coyle, H. Drevermann, A. Engelhardt, R.W. Forty, M. Frank, M. Girone, R. Hagelberg, J. Harvey, R. Jacobsen,[24] P. Janot, B. Jost, J. Knobloch, I. Lehraus, M. Maggi, C. Markou,[23] E.B. Martin, P. Mato, H. Meinhard, A. Minten, R. Miquel, T. Oest, P. Palazzi, J.R. Pater, P. Perrodo, J.-F. Pusztaszeri, F. Ranjard, P. Rensing, L. Rolandi, D. Schlatter, M. Schmelling, O. Schneider, W. Tejessy, I.R. Tomalin, A. Venturi, H. Wachsmuth, W. Wiedenmann, T. Wildish, W. Witzeling, J. Wotschack

European Laboratory for Particle Physics (CERN), 1211 Geneva 23, Switzerland

Z. Ajaltouni, M. Bardadin-Otwinowska,[2] A. Barres, C. Boyer, A. Falvard, P. Gay, C. Guicheney, P. Henrard, J. Jousset, B. Michel, S. Monteil, J-C. Montret, D. Pallin, P. Perret, F. Podlyski, J. Proriol, J.-M. Rossignol, F. Saadi

Laboratoire de Physique Corpusculaire, Université Blaise Pascal, IN^2P^3-CNRS, Clermont-Ferrand, 63177 Aubière, France

T. Fearnley, J.B. Hansen, J.D. Hansen, J.R. Hansen, P.H. Hansen, B.S. Nilsson

Niels Bohr Institute, 2100 Copenhagen, Denmark[9]

A. Kyriakis, E. Simopoulou, I. Siotis, A. Vayaki, K. Zachariadou

Nuclear Research Center Demokritos (NRCD), Athens, Greece

A. Blondel,[21] G. Bonneaud, J.C. Brient, P. Bourdon, L. Passalacqua, A. Rougé, M. Rumpf, R. Tanaka, A. Valassi, M. Verderi, H. Videau

Laboratoire de Physique Nucléaire et des Hautes Energies, Ecole Polytechnique, IN^2P^3-CNRS, 91128 Palaiseau Cedex, France

D.J. Candlin, M.I. Parsons

Department of Physics, University of Edinburgh, Edinburgh EH9 3JZ, United Kingdom[10]

E. Focardi, G. Parrini

Dipartimento di Fisica, Università di Firenze, INFN Sezione di Firenze, 50125 Firenze, Italy

M. Corden, M. Delfino,[12] C. Georgiopoulos, D.E. Jaffe

Supercomputer Computations Research Institute, Florida State University, Tallahassee, FL 32306-4052, USA [13,14]

A. Antonelli, G. Bencivenni, G. Bologna,[4] F. Bossi, P. Campana, G. Capon, F. Cerutti, V. Chiarella, G. Felici, P. Laurelli, G. Mannocchi,[5] F. Murtas, G.P. Murtas, M. Pepe-Altarelli

Laboratori Nazionali dell'INFN (LNF-INFN), 00044 Frascati, Italy

S.J. Dorris, A.W. Halley, I. ten Have,[6] I.G. Knowles, J.G. Lynch, W.T. Morton, V. O'Shea, C. Raine, P. Reeves, J.M. Scarr, K. Smith, M.G. Smith, A.S. Thompson, F. Thomson, S. Thorn, R.M. Turnbull

Department of Physics and Astronomy, University of Glasgow, Glasgow G12 8QQ,United Kingdom[10]

U. Becker, O. Braun, C. Geweniger, G. Graefe, P. Hanke, V. Hepp, E.E. Kluge, A. Putzer, B. Rensch, M. Schmidt, J. Sommer, H. Stenzel, K. Tittel, S. Werner, M. Wunsch

Institut für Hochenergiephysik, Universität Heidelberg, 69120 Heidelberg, Fed. Rep. of Germany[16]

R. Beuselinck, D.M. Binnie, W. Cameron, D.J. Colling, P.J. Dornan, N. Konstantinidis, L. Moneta, A. Moutoussi, J. Nash, G. San Martin, J.K. Sedgbeer, A.M. Stacey

Department of Physics, Imperial College, London SW7 2BZ, United Kingdom[10]

G. Dissertori, P. Girtler, E. Kneringer, D. Kuhn, G. Rudolph

Institut für Experimentalphysik, Universität Innsbruck, 6020 Innsbruck, Austria[18]

C.K. Bowdery, T.J. Brodbeck, P. Colrain, G. Crawford, A.J. Finch, F. Foster, G. Hughes, T. Sloan, E.P. Whelan, M.I. Williams

Department of Physics, University of Lancaster, Lancaster LA1 4YB, United Kingdom[10]

A. Galla, A.M. Greene, K. Kleinknecht, G. Quast, J. Raab, B. Renk, H.-G. Sander, R. Wanke, C. Zeitnitz

Institut für Physik, Universität Mainz, 55099 Mainz, Fed. Rep. of Germany[16]

J.J. Aubert, A.M. Bencheikh, C. Benchouk, A. Bonissent, G. Bujosa, D. Calvet, J. Carr, C. Diaconu, F. Etienne, M. Thulasidas, D. Nicod, P. Payre, D. Rousseau, M. Talby

Centre de Physique des Particules, Faculté des Sciences de Luminy, IN^2P^3-CNRS, 13288 Marseille, France

I. Abt, R. Assmann, C. Bauer, W. Blum, D. Brown,[24] H. Dietl, F. Dydak,[21] C. Gotzhein, K. Jakobs, H. Kroha, G. Lütjens, G. Lutz, W. Männer, H.-G. Moser, R. Richter, A. Rosado-Schlosser, R. Settles, H. Seywerd, U. Stierlin,[2] R. St. Denis, G. Wolf

Max-Planck-Institut für Physik, Werner-Heisenberg-Institut, 80805 München, Fed. Rep. of Germany[16])

R. Alemany, J. Boucrot, O. Callot, A. Cordier, F. Courault, M. Davier, L. Duflot, J.-F. Grivaz, Ph. Heusse, M. Jacquet, D.W. Kim,[19] F. Le Diberder, J. Lefrançois, A.-M. Lutz, G. Musolino, I. Nikolic, H.J. Park, I.C. Park, M.-H. Schune, S. Simion, J.-J. Veillet, I. Videau

Laboratoire de l'Accélérateur Linéaire, Université de Paris-Sud, IN^2P^3-CNRS, 91405 Orsay Cedex, France

D. Abbaneo, P. Azzurri, G. Bagliesi, G. Batignani, S. Bettarini, C. Bozzi, G. Calderini, M. Carpinelli, M.A. Ciocci, V. Ciulli, R. Dell'Orso, R. Fantechi, I. Ferrante, L. Foà,[1] F. Forti, A. Giassi, M.A. Giorgi, A. Gregorio, F. Ligabue, A. Lusiani, P.S. Marrocchesi, A. Messineo, G. Rizzo, G. Sanguinetti, A. Sciabà, P. Spagnolo, J. Steinberger, R. Tenchini, G. Tonelli,[26] G. Triggiani, C. Vannini, P.G. Verdini, J. Walsh

Dipartimento di Fisica dell'Università, INFN Sezione di Pisa, e Scuola Normale Superiore, 56010 Pisa, Italy

A.P. Betteridge, G.A. Blair, L.M. Bryant, Y. Gao, M.G. Green, D.L. Johnson, T. Medcalf, Ll.M. Mir, J.A. Strong

Department of Physics, Royal Holloway & Bedford New College, University of London, Surrey TW20 OEX, United Kingdom[10]

V. Bertin, D.R. Botterill, R.W. Clifft, T.R. Edgecock, S. Haywood, M. Edwards, P. Maley, P.R. Norton, J.C. Thompson

Particle Physics Dept., Rutherford Appleton Laboratory, Chilton, Didcot, Oxon OX11 OQX, United Kingdom[10]

B. Bloch-Devaux, P. Colas, H. Duarte, S. Emery, W. Kozanecki, E. Lançon, M.C. Lemaire, E. Locci, B. Marx, P. Perez, J. Rander, J.-F. Renardy, A. Rosowsky, A. Roussarie, J.-P. Schuller, J. Schwindling, D. Si Mohand, A. Trabelsi, B. Vallage

CEA, DAPNIA/Service de Physique des Particules, CE-Saclay, 91191 Gif-sur-Yvette Cedex, France[17]

R.P. Johnson, H.Y. Kim, A.M. Litke, M.A. McNeil, G. Taylor

Institute for Particle Physics, University of California at Santa Cruz, Santa Cruz, CA 95064, USA[22]

A. Beddall, C.N. Booth, R. Boswell, S. Cartwright, F. Combley, I. Dawson, A. Koksal, M. Letho, W.M. Newton, C. Rankin, L.F. Thompson

Department of Physics, University of Sheffield, Sheffield S3 7RH, United Kingdom[10]

A. Böhrer, S. Brandt, G. Cowan, E. Feigl, C. Grupen, G. Lutters, J. Minguet-Rodriguez, F. Rivera,[25] P. Saraiva, L. Smolik, F. Stephan

Fachbereich Physik, Universität Siegen, 57068 Siegen, Fed. Rep. of Germany[16]

L. Bosisio, R. Della Marina, G. Ganis, G. Giannini, B. Gobbo, L. Pitis, F. Ragusa[20]

Dipartimento di Fisica, Università di Trieste e INFN Sezione di Trieste, 34127 Trieste, Italy

J. Rothberg, S. Wasserbaech

Experimental Elementary Particle Physics, University of Washington, WA 98195 Seattle, U.S.A.

S.R. Armstrong, L. Bellantoni, P. Elmer, Z. Feng, D.P.S. Ferguson, Y.S. Gao, S. González, J. Grahl, J.L. Harton, O.J. Hayes, H. Hu, P.A. McNamara III, J.M. Nachtman, W. Orejudos, Y.B. Pan, Y. Saadi, M. Schmitt, I.J. Scott, V. Sharma, J.D. Turk, A.M. Walsh, F.V. Weber,[1] Sau Lan Wu, X. Wu, J.M. Yamartino, M. Zheng, G. Zobernig

Department of Physics, University of Wisconsin, Madison, WI 53706, USA[11]

1   Introduction

The reaction $\gamma\gamma \to Q\bar{Q}$ where Q is a heavy quark (charm or beauty) has a number of favourable aspects as a test of QCD when compared to other $\gamma\gamma$ processes[1, 2]. Firstly the theoretical uncertainties are reduced somewhat as the quark mass sets the scale for the strong interaction. Secondly there is concluded to be negligible background from the soft process of Vector Meson Dominance (VMD) based on observations of collisions of real and virtual photons on a proton target [3]. As a check of this conclusion the PYTHIA Monte Carlo [4] was used to calculate the rate of production of charmed mesons via VMD in $\gamma\gamma$ collisions in which one of the photons has fluctuated into a J/Ψ. The predicted cross section is negligible compared to the rates from hard processes, generally referred to in the following as QCD. Figure 1 shows some of the diagrams contributing to heavy quark production in two-photon physics. Diagrams (a)-(c) are examples of the so-called direct process in which the photon couples directly to a quark. Diagram (a) is the Born term direct process which is equivalent to the Quark Parton Model (QPM), (b) and (c) are virtual and real QCD corrections to the Born term. At low beam energy this direct process is completely dominant, however at high beam energies there is predicted to be a large contribution from the 'single resolved photon' processes depicted in diagrams (d)-(f) [1, 2]. The largest part of the resolved process is given by the photon-gluon fusion process; this property offers the possibility of measuring the gluon content of the photon which is currently poorly known. Doubly resolved processes have been calculated to give a negligible contribution for presently available beam energies [1].
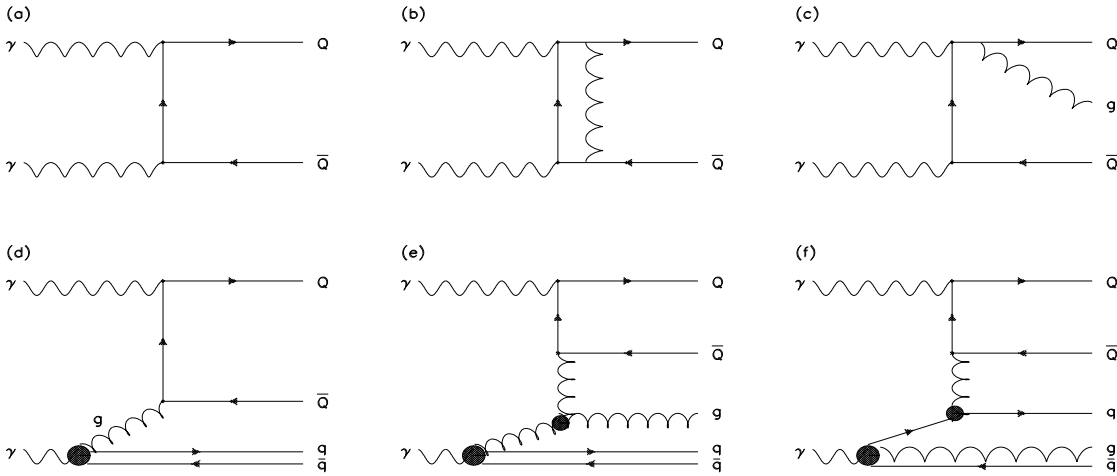
Figure 1: Examples of diagrams contributing to heavy quark production in $\gamma\gamma$ collisions. (a) Direct contribution: Born term (QPM); (b) virtual correction to direct term; (c) real correction to direct process; (d),(e),(f) 'resolved' contributions.

Experimental measurements of charm production in $\gamma\gamma$ physics have generally been made by observing the production of D^{*+} particles [1] . Early measurements were reported by JADE [5], TPC/Two-Gamma[6], and TASSO[7]. Recently results have also been produced by TOPAZ[8, 9]. These results are summarised in Table 1, the last column of which shows the total cross sections for $\sigma(e^+e^- \to e^+e^-$ D^{*+}X) calculated by applying various adjustments to the published results. For TPC/Two-Gamma[6], JADE[5], TASSO[7] and the earlier TOPAZ result[8], this adjustment accounts for the latest values for the D^{*+} and

---

[1] Throughout this paper charge conjugate decays are implicitly included.

1

Experiment	Beam energy (GeV)	$\sigma(e^+e^- \to e^+e^- \mathrm{D}^{*+} \mathrm{X})$ pb	
		published	adjusted
TPC/Two-Gamma[6]	14.5	74 ± 32	56 ± 24
JADE[5].	17	-	173 ± 70
TASSO[7]	17	97 ± 29	68 ± 20
TOPAZ$^{(1)}$[8]	29	75 ± 25	163 ± 54
TOPAZ$^{(2)}$[9]	29	23.5 ± 4.6	196 ± 35

Table 1: Measurements of D^{*+} production in two photon physics. Where a cross section has been published it is given in the third column. In the fourth column is shown the results of a calculation of the total cross section after applying various adjustments as described in the text.

D^0 branching ratios [10]. The two TOPAZ cross sections are with the additional conditions (1) $p_\mathrm{t}^{\mathrm{D}^{*+}} > 1.6\,\mathrm{GeV/c}$ and (2) $p_\mathrm{t}^{\mathrm{D}^{*+}} > 1.6\,\mathrm{GeV/c}$, $|\cos(\theta)| < 0.77$. A total cross section was obtained from the published figures by multiplying the total QPM cross section by the ratio of the observed cross section to the QPM cross section for the same acceptance.

In this paper the process $\gamma\gamma \to c\bar{c}$ is measured at a beam energy of 45 GeV via the inclusive production of D^{*+} mesons, which are detected in their decay to $\mathrm{D}^0\pi^+$ with the D^0 being observed in the decay modes (1) $\mathrm{K}^-\pi^+$, (2) $\mathrm{K}^-\pi^+\pi^0$ and (3) $\mathrm{K}^-\pi^+\pi^-\pi^+$. In most previous studies only a QPM model was available, so results are included in this study using both QPM and QCD Monte Carlo programs to allow comparisons between the two.

2 Experimental Procedure

The first stage of the analysis consisted of the selection of a low background sample of events of the type $\gamma\gamma \to$ hadrons from the 73 pb^{-1} of data collected by ALEPH in the period 1990-93. The ALEPH detector has been described in detail in Ref. [11]. The critical part of the detector for this analysis is the large Time Projection Chamber (TPC), a cylindrical, three-dimensional imaging drift chamber covering radii from 30 to 180 cm from the beam. For charged tracks with $|\cos(\theta)| < 0.97$ it can provide up to 21 space point measurements, and up to 338 measurements of the ionization loss (dE/dx) which enables particle identification to be performed. The Inner Tracking Chamber (ITC) is a cylindrical multiwire drift chamber which covers the region from 16 to 26 cm from the beam and can give up to 8 additional points for tracks with $|\cos(\theta)| < 0.97$. In 1991 a silicon vertex detector was installed and can measure two additional points for tracks with $|\cos(\theta)| < 0.65$. The transverse momentum resolution of charged tracks Δp_t is given by the formula

$$(\Delta p_\mathrm{t}/p_\mathrm{t})^2 = (\alpha \times 10^{-3} p_\mathrm{t}(\mathrm{GeV/c}))^2 + (0.005)^2$$

where the value of α is 1.2 when tracks are measured using the TPC alone, 0.8 when the ITC is added, and 0.6 when points from all three tracking detectors are available.

Surrounding the TPC is the e/γ calorimeter (ECAL) consisting of a highly segmented sandwich of wire chambers and lead plates covering the polar angle region $|\cos(\theta)| < 0.98$. Position and energy of electromagnetic showers are measured using $3 \times 3\,\mathrm{cm}^2$ cathode pads read out in three sections in depth, a feature which enables electromagnetic and hadronic showers to be distinguished by their differing shower profiles. The energy resolution for electromagnetic showers is given by $\Delta E/E = 0.18/\sqrt{E} + 0.009$ (E in GeV). The

event selection was based on "Energy Flow Objects" [12] which consist of charged tracks and neutral clusters.

In order to reject events due to decays of the Z the following cuts were applied:

- Total charged energy < 20 GeV;
- Number of charged tracks > 3;
- Number of charged tracks < (40 - visible energy in GeV);
- $p_{\rm t}^{\rm tot} < 8.0\,{\rm GeV}/c$, where $p_{\rm t}^{\rm tot}$ is the transverse component with respect to the beam direction of the vector sum of the momenta of all Energy Flow Objects;
- Visible Invariant Mass (W_{vis}) between 4.0 and 45 GeV$/c^2$;
- A vertex position within 14 cm in z and 10 cm in r from the interaction point.

This selection produced a sample of 134960 events.

3   Measurement of D^{*+} Meson Production

The technique to extract a signal for charm exploits the fact that the available kinetic energy in the decay $D^{*+} \to D^0 \pi^+$ is only 6 MeV. The signal is typically displayed by plotting $\Delta M = M_{D^{*+}} - M_{D^0}$ for all reconstructed decay product candidates. A D^0 decay mode can be used in this analysis if it has a reasonable branching ratio (at least of order 1%) together with the possibility of accurately reconstructing all the decay products; for example, semi-leptonic decays cannot be used due to the undetected neutrino. For the current study a D^0 is reconstructed in its decays to (1)$K^- \pi^+$, (2) $K^- \pi^+ \pi^0$, and (3) $K^- \pi^+ \pi^+ \pi^-$. Having formed a candidate D^0 meson, which is within the accepted mass range, tracks identified as pions are added in turn to form candidate D^{*+} mesons, ΔM being determined in each case. For background tracks the spectrum rises from a kinematic lower limit of 139.6 MeV$/c^2$ (M_{π^+}), whilst the signal produces a peak at 145.5 MeV$/c^2$, i.e. $M_{D^{*+}} - M_{D^0}$, which is a region where the background is small.

Each charged track of each surviving event is considered in turn as a kaon and/or pion candidate. The kaon/pion identification is provided by the dE/dx information. The track is flagged as a kaon if the dE/dx probability is greater than 10% for a kaon mass hypothesis. Independently, if the probability is greater than 0.5% for a pion mass hypothesis then the track is flagged as a pion (the same track may be flagged as a kaon, pion, both or neither). Candidate D^0 are formed by taking relevant combinations of identified kaons and pions which have an invariant mass within the accepted range around M_{D^0}. Remaining pions, which have opposite charge to that of the kaon, are added in turn to the D^0 to form D^{*+} candidates. To reduce the combinatorial backgrounds from soft processes, two further cuts are applied to the D^{*+}, namely it must have $|\cos(\theta)| < 0.875$, and $|p_{\rm t}| >$ 2.0 GeV/c (θ is the polar angle relative to the e$^+$ beam direction).

Details specific to each decay mode are described below. The resulting mass difference distributions are shown in Fig. 2. The mass difference, ΔM, is also shown for a 'wrong sign' combination of tracks, constructed by requiring the pion used to form the D^{*+} from the D^0 to have the same charge as the kaon. This produces a background spectrum from which the significance of the signal obtained from the right sign combination may be extracted. The mass range around the D^0 mass is trebled when forming the wrong sign signal in order to increase the statistical significance of the background measurement. It is possible for there to be several entries per event in the mass difference plot. However, it is found in practice that no event gives multiple entries in the signal region.
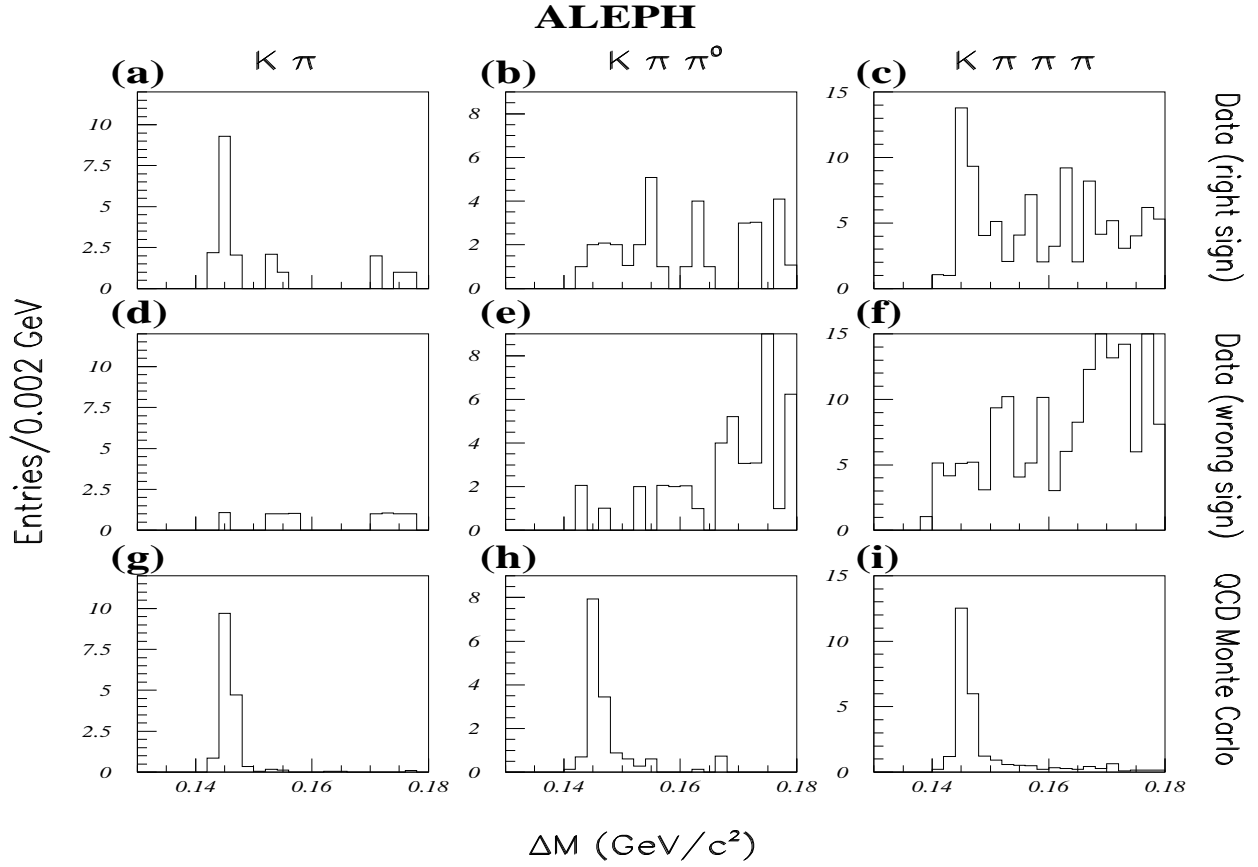
ALEPH

Figure 2: $\Delta M (= M_{D^{*+}} - M_{D^0})$ in GeV/c^2. Data are shown for the decay chain: $D^{*+} \to D^0 \pi^+$, followed by (a) $D^0 \to K^- \pi^+$, (b) $D^0 \to K^- \pi^+ \pi^0$, (c) $D^0 \to K^- \pi^+ \pi^+ \pi^-$. The wrong-sign background are seen in the same channels in plots (d)-(f). The plots (g)-(i) show the normalized distributions from the QCD Monte Carlo.

3.1 Mode (1) $D^0 \to K^- \pi^+$

Candidate D^0 mesons are reconstructed by considering all combinations of oppositely charged kaon and pion pairs. Such a combination is retained if it has an invariant mass within the range $1.85 \, \text{GeV/c}^2 < M_{K^- \pi^+} < 1.88 \, \text{GeV/c}^2$ which was determined from the resolution observed in the Monte Carlo detector simulation.

3.2 Mode (2) $D^0 \to K^- \pi^+ \pi^0$

π^0 candidates are formed from pairs of photons with energy greater than 250 MeV identified in the ECAL and the invariant mass of the pair, $M_{\gamma\gamma}$, is calculated. The energy resolution of genuine π^0 is improved by a constrained fit of the photon energies to the π^0 mass. This improves the energy resolution on average by a factor of two. The candidate π^0 is retained if the probability that the two photons came from a π^0 is greater than 5% and the π^0 has $|\cos(\theta)| < 0.93$.

From the identified kaons and pions all combinations of the form $K^- \pi^+ \pi^0$ are considered and accepted as D^0 candidates provided the mass is within the range $1.83 \, \text{GeV/c}^2 < M_{K^- \pi^+ \pi^0} < 1.90 \, \text{GeV/c}^2$. This mass window is again determined from the Monte Carlo resolution.

3.3 Mode (3) $D^0 \to K^- \pi^+ \pi^+ \pi^-$

By fitting the four tracks in a candidate D^0 to a common vertex with loose constraints the background in this mode is reduced by 10%. The range $1.84\,\text{GeV/c}^2 < M_{K^- \pi^+ \pi^+ \pi^-} < 1.88\,\text{GeV/c}^2$ was used to select D^0 candidates.

3.4 Selection Efficiency

Selection efficiencies were measured by passing samples of Monte Carlo events through the detector simulation and reconstruction programs. Two separate programs have been used. The first one simulates the QPM production of charm quarks using the program of J.A.M. Vermaseren[13]. The second program has been developed in collaboration with the authors of Ref. [1] and produces events according to their QCD calculation. In both cases the charm quarks are fragmented by the JETSET program[4]. Separate samples were produced for each of the three decay chains where one quark is required to have produced a D^{*+}, with the subsequent decay $D^{*+} \to D^0 \pi^+, D^0 \to$ modes 1,2 and 3. The 'other' quark is then free to fragment according to known charm branching ratios. The events have been corrected for trigger efficiency as described in Ref. [14]; for all events in the signal region the trigger efficiency is close to 100%.
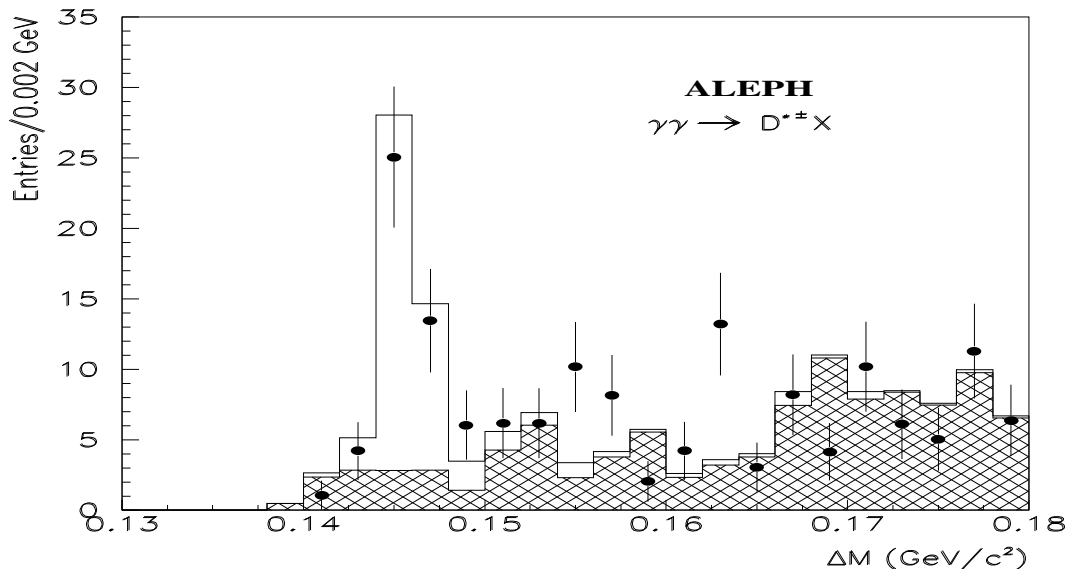

Figure 3: The charm signal in $\gamma\gamma$ events obtained by plotting $\Delta M = M_{D^{*+}} - M_{D^0}$ for the sum of the three channels studied. The points are the data with statistical errors only. The histogram shows the result of a fit to the sum of the predicted QCD signal and the background shape (shown as the shaded area) obtained from wrong-sign events.

4 Results

In order to measure the size of the signal, all of the three channels studied were combined. The signal region was taken as $0.144 < \Delta M < 0.148\,\text{GeV/c}^2$. To find the size of the background under the peak in this region it was necessary to allow for the fact that the mass window around the D^0 was enlarged in the 'wrong sign' sample. To account for this a maximum likelihood fit was performed on the data in the range $0.13 < \Delta M <$

$0.18 \, \text{GeV}/c^2$, wherein the Monte Carlo was used to give the expected shape for the peak and the wrong sign data was used to give the shape for the background. Figure 3 shows the combined data signal with the fitted signal and background distributions.

The only source of background that can contribute to the signal is contamination from e^+e^- annihilation events. A Monte Carlo study using PYTHIA [4] showed this to be negligible.

The size of systematic errors resulting from the use of the detector simulation to calculate selection efficiencies was calculated by varying the resolution of a number of parameters critical to the analysis. This variation was within a range that was consistent with the observed agreement between data and Monte Carlo in our large sample of e^+e^- annihilation events. The parameters used were dE/dx, D^0 mass, and visible energy . The result of this study is summarized in Table 2. Combining these errors in quadrature results in a total systematic error on the selection efficiency of 13%. Thus the number of D^{*+} found in the data is 33 ± 7 (stat) ± 4 (sys).

systematic effect	uncertainty
dE/dx resolution	9 %
D^0 mass resolution	6%
visible energy	7 %
Total	13 %

Table 2: Contributions to the systematic error on selection efficiency.

The calculation of the theoretical expectation is discussed in two parts, first the process $e^+e^- \to e^+e^- \, D^{*+} X \, (D^{*+} \to D^0 \pi)$ is considered, and then the number of events expected to be observed in any given D^0 channel is calculated. $N_{D^{*+} \to D^0 \pi}$, the number of D^{*+} produced in the data which subsequently decay to $D^0 \pi^+$ is given by the formula:

$$N_{D^{*+} \to D^0 \pi} = 2 \times \sigma(e^+e^- \to e^+e^- c\bar{c}) \times \mathcal{L} \times P_{c \to D^{*\pm}} \times B_*$$

where:

- $\sigma(e^+e^- \to e^+e^- c\bar{c})$ is the cross section for $e^+e^- \to e^+e^- c\bar{c}$ for which the final state has a mass greater than $3.8 \, \text{GeV}/c^2$ and was calculated using a program supplied by the authors of Ref. [1]. To determine the theoretical error the charm quark mass was varied between 1.3 and $1.7 \, \text{GeV}/c^2$ and the QCD energy scale was allowed to vary between m_Q and $2 \, m_Q$, where m_Q is the heavy quark mass. The dominant source of uncertainty is the former.
- $\mathcal{L}$ is the integrated luminosity of the data ($73.4 \, \text{pb}^{-1}$).
- $P_{c \to D^{*\pm}}$ is the fraction of charm quarks hadronizing into a charged D^*, and B_* is the branching fraction $B(D^{*+} \to D^0 \pi)$. Equation (4) of Ref. [15] gives the combined probability

$$P_{c \to D^{*\pm}} \times B_* \times B_0 = (6.5 \pm 0.5 \, (\text{stat.}) \pm 0.2 \, (\text{syst.})) \times 10^{-3},$$

where B_0 is the branching fraction for $D^0 \to K^- \pi^+$. Dividing by $4.01 \pm 0.14\%$, which is the value for B_0 given in Ref. [10], gives $P_{c \to D^{*\pm}} \times B_* = 0.162 \pm 0.0144$.

The result of this calculation is summarised in Table 3.

6

Process	Number of decays	Graphs of Figure 1
QPM	5166 ± 1001	1(a)
QCD ('direct')	6476 ± 1081	1(a),1(b),1(c)
QCD ('resolved')	4944 ± 2244	1(d),1(e),1(f)

Table 3: Predicted total number of $D^{*+} \rightarrow D^0\pi$ decays in events of the type $e^+e^- \rightarrow e^+e^-D^{*+}X$; the error is dominated by the charm mass uncertainty.

The expectation for any given decay channel in the data is then obtained from the above figures by multiplying by the selection efficiency measured in the Monte Carlo and the branching fractions given by the Particle Data Group [10]. These values are summarised in Table 4. The total number of events expected is 28±6 for QPM or 46±11 for QCD which includes direct and resolved contributions, to be compared with the observed number of 33 ± 7 (stat) ± 4 (sys), the systematic error being due to selection efficiencies (Table 2).

Using the branching fraction for D^{*+} to $D^0\pi^+$ (68.1±1.3% [10]) enables the result to be expressed as a cross section. When the QCD model is used to calculate selection efficiencies the result is

$$\sigma(e^+e^- \rightarrow e^+e^-\ D^{*+}X) = 155 \pm 33\,(\text{stat})\ \pm 21\,(\text{sys})\,\text{pb}$$

whereas using the QPM model gives a lower cross section

$$\sigma(e^+e^- \rightarrow e^+e^-\ D^{*+}X) = 121 \pm 26\,(\text{stat})\ \pm 16\,(\text{sys})\,\text{pb}.$$

This difference is largely due to the lower selection efficiency for the single resolved processes (Figure 1 (d)-(f)). The systematic error includes the contributions from the selection efficiency and branching fractions added in quadrature. These values are compatible with both the QPM (100 ± 20 pb) and QCD (220 ± 60 pb) predictions.

Process	D^0 decay mode	Branching Fraction	Selection Efficiency	Predicted Number of D^{*+}
QPM	$K^+\pi^-$	0.0401 ± 0.0014	0.046	9.5 ± 1.9
	$K^+\pi^-\pi^0$	0.138 ± 0.010	0.009	6.4 ± 1.3
	$K^+\pi^-\pi^+\pi^+$	0.081 ± 0.005	0.029	12.1 ± 2.5
QCD direct	$K^+\pi^-$	0.0401 ± 0.0014	0.041	10.6 ± 1.8
	$K^+\pi^-\pi^0$	0.138 ± 0.010	0.011	9.8 ± 1.8
	$K^+\pi^-\pi^+\pi^+$	0.081 ± 0.005	0.027	14.2 ± 2.5
QCD resolved	$K^+\pi^-$	0.0401 ± 0.0014	0.022	4.4 ± 2.0
	$K^+\pi^-\pi^0$	0.138 ± 0.010	0.004	2.6 ± 1.2
	$K^+\pi^-\pi^+\pi^+$	0.081 ± 0.005	0.012	4.8 ± 2.2

Table 4: Calculation of expected number of observed D^0 decays.

More information can be gained by studying distributions of events after background subtraction in the D^{*+} signal region and comparing to the predictions of QCD and QPM. Around 50% of the QCD events contain additional partons, which should be reflected in
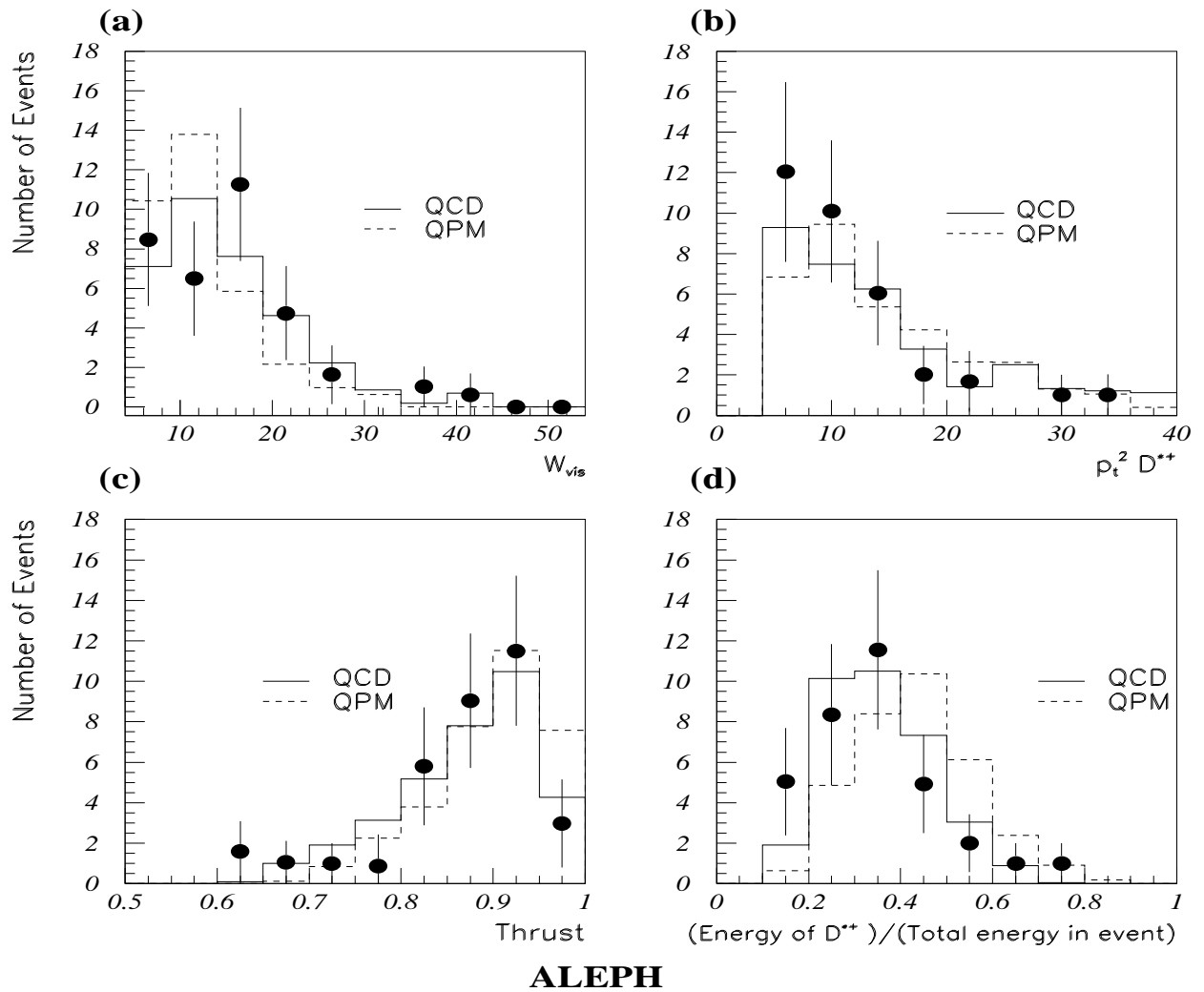
(a)

(b)

(c)

(d)

ALEPH

Figure 4: Distributions for events containing a D^{*+} (background subtracted) (a) W_{vis} (b) p_t^2 of D^{*+} (c) Thrust (d) Energy of the D^{*+} / Total energy in event. The error bars are statistical and systematic errors added in quadrature.

the final state. Shown in Fig. 4 are the following distributions that would be expected to show differences due to the presence of additional partons in the final state: the visible invariant mass of the event (W_{vis}), p_t^2 of the D^{*+}, the thrust of the event and the energy of the D^{*+} divided by the total energy in the event. The models have each been renormalised to the same number of events as the data, which is equivalent to using a charm mass of $1.9\,\mathrm{GeV}/c^2$ in the case of QCD, and $1.4\,\mathrm{GeV}/c^2$ for QPM. A quantitative comparison has been made using the Kolmogorov test which gives the probability that two histograms come from the same parent distribution. All distributions favour the QCD prediction. The most significant comparison is given by Figure 4(d) for which a probability of 0.87 is found when comparing QCD to the data but 10^{-4} for QPM.

5   Conclusions

The first measurement of the cross section for $D^{*\pm}$ production in $\gamma\gamma$ collisions at LEP I beam energies has been made. The value is consistent with both the QCD and QPM predictions. Comparison of various distributions in the data to QCD and QPM Monte Carlo models favours the former. The QCD model is therefore used to calculate

the selection efficiency and extract the final result

$$\sigma(e^+e^- \to e^+e^- \, D^{*\pm}X) = 155 \pm 33 \, (\text{stat}) \pm 21 \, (\text{sys}) \, \text{pb}.$$

Figure 5 shows the result compared to other measurements and to the predictions of Ref. [1]. This results falls at the low end of the range of QCD predictions, in contrast with earlier measurements which have tended to lie towards higher values.

6 Acknowledgements

We would like to thank our colleagues of the accelerator divisions at CERN for the outstanding performance of the LEP machine. Thanks are also due to the many engineers, and technical personnel at CERN and at the home institutes for their contribution to ALEPH's success. Those of us not from member states wish to thank CERN for its hospitality. We would like to thank M.Krämer, P.M.Zerwas, and J.Zunft, for their help in developing the QCD generator used in this study.
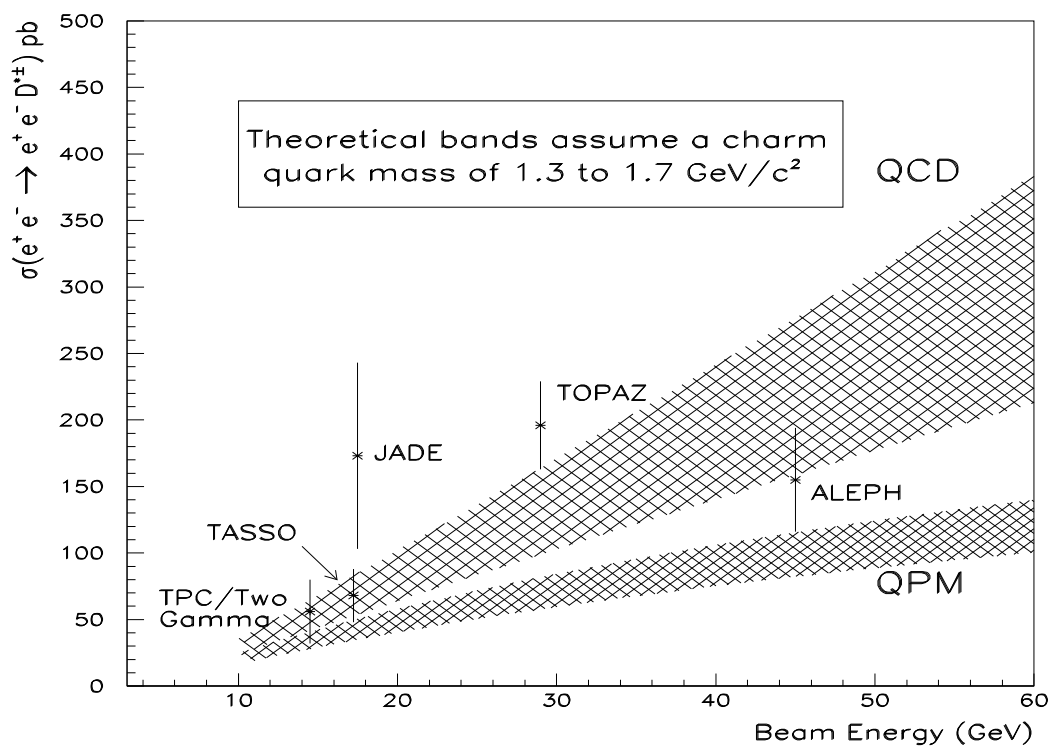

Figure 5: Comparison of measured cross sections [5,6,7,9] for $e^+e^- \to e^+e^- \, D^{*+}X$ (Table 1) to theoretical predictions from Ref. [1].

References

[1] M. Drees, M. Krämer, J. Zunft and P.M. Zerwas, Phys. Lett. B 306 (1993) 371.

[2] M. Drees and R. Godbole, Nucl. Phys. B 339 (1990) 355.

[3] D. Aston et al., Phys. Lett. B 94 (1980) 113;
J.J. Aubert et al., Nucl. Phys. B 213 (1983) 1;
J.J. Aubert et al., Nucl. Phys. B 213 (1983) 31.

[4] T. Sjöstrand, Computer Physics Commun. 82 (1994) 74.

[5] JADE Collab., W. Bartel et al. , Phys. Lett. B184 (1987) 288;
A.J. Finch in Proceedings of the VIII International Workshop on Photon-Photon Collisions, Shoresh, Israel (1988), U. Karshon ed. (World Scientific), p. 75;
The selection efficiences were 0.31% for the $K^+\pi^-\pi^0$ channel and 0.27% in the $K^+\pi^-\pi^0\pi^0$ channel (J.M. Nye, private communication).

[6] TPC/2γ Collab., M. Alston-Garnjost et al. Phys. Lett. B 252 (1990) 499.

[7] TASSO Collab., W. Braunschweig et al., Z.Phys. C 47 (1990) 499.

[8] TOPAZ Collab., R.Enomoto et al. Phys. Rev. D 50 (1994) 1879.

[9] TOPAZ Collab., R.Enomoto et al. Phys. Lett. B 328 (1994) 535.

[10] L. Montanet et al. (Particle Data Group), Phys. Rev. D 50, Part 1 (1994).

[11] ALEPH Collab., D. Decamp et al., Nucl. Instr. Meth. A 294 (1990) 121.

[12] ALEPH Collab., D. Buskulic et al., CERN-PPE/94-170.

[13] J.A.M. Vermaseren, in: Procn. of the IV Intern. Workshop on Gamma Gamma Interactions, eds. G. Cochard and P. Kessler (1980);
Long program write up by J.A.M. Vermaseren (unpubl.).

[14] ALEPH Collab., D. Buskulic et al., Phys. Lett. B 313 (1993) 509.

[15] ALEPH Collab., D. Buskulic et al., Z. Phys. C 62, 1 (1994).